

Chapter 4

Optimal Summation of Natural Power Resources in Microgrid

4.1 Introduction

Due to the beginning of the electrical energy market, the restructuring of the electrical power industry has taken place rapidly. Simultaneously, awareness about global warming is encouraged to reduce pollution and committed to using natural resources in the power system. The development of microgrids with the integration of natural sources is getting more attraction in power society. However, microgrids' planning, operation, and management face many technical and economic issues. The standard low-voltage distribution structures are formed explicitly with the aid of the interconnection of small energy assets, along with MGT, small WT, DG, PV cells, and fuel cells, with loads and controllable storage devices such as flywheels, supercapacitors, and batteries [7]. This low- medium voltage distribution system named microgrid can be operated in grid-connected mode, and stand-alone mode [85],[86]. The clear microgrid concept, including microgrid structure, control, protection, and economics, has been presented in the report [87] which is about the integration of distributed energy resources. The team of DNV KEMA Energy and sustainability and the Peregrine Energy Group have presented one study report in which a clear definition of a microgrid has been established [88]. The detailed definition of a microgrid has been given as follows:

A power distribution network comprising multiple electric loads and distributed energy resources is characterized by all of the following:

- The ability to operate independently or in conjunction with a microgrid;
- One or more points of common coupling (PCC's) to the microgrid;
- The network should have the ability to operate all distributed energy resources (DER), including load and energy storage components, in a controlled and coordinated fashion, either while connected to the maingrid or operating independently.
- The network should have the ability to interact with the microgrid in real time and thereby optimize system performance and operational savings.

This report focuses on the primary advantages of microgrids. The primary benefits identified by the study team are the ability to provide electricity to critical loads within the microgrid economically, as well as to improve power quality, flexibility, and reliability by integrating and optimizing various energy sources. Therefore, microgrids represent coordinated control of DERs in order to optimize economics, reliability, and clean energy (if possible), as well as to stabilize electric loads and generation while operating independently of the grid. This report contains details on various pilot microgrid activities taking place in the United States and Europe. Four microgrid business models have been investigated to address potential conflicts with traditional distribution utility business models: distribution company microgrid, single-user microgrid, hybrid microgrid, and multi-user microgrid. To take advantage of what microgrids offer, the distribution grid network should be updated by deploying clean and renewable energy systems.

The prime technical issues relevant to microgrids have been explored in [87]. The white paper has covered contextual information and microgrid background along with control strategy requirements for the effective functionality of grid-connected microgrid and island microgrid. The protection and safety issues which may be implementable in MicroGrids have been addressed for reliable power. The configuration and operation of microgrid have been dictated by discussion of fundamental economical questionnaires and generation technology. Policy and planning direction in relation to microgrids has been suggested in the research project report for the Commonwealth of Massachusetts on the subject of microgrids [88]. In accordance with microgrid goals, a set of recommendations for emergency preparedness, greenhouse gas reductions, smart grid implementation, and public safety have been made. Installing distributed energy resources (DER) as well as emerging control and communication technology on the distribution side to operate the

distribution system as a coordinated, stable, and islandable/grid-connected microgrid. This microgrid could provide benefits in terms of clean energy.

In the first decade of the 21st century, many research projects on the design, operation, and control of microgrids in various regions of the world, such as the MICROGRID project of Europe [89], the CERTS microgrid in USA [90], and new energy integration test project by NEDO in Japan [91] have been carried out. At present numerous incentives have been offered for a microgrid projects in many states and countries of the world. The various program regarding optimal planning and operation of microgrid, Energy management system (EMS) of microgrid have been proposed to derive the greatest profit from the configuration of microgrid, increase the efficiency of natural power DG usage, and optimize the economic operation of microgrid. The primary functions of optimal planning and operation of a microgrid are minimizing cost and losses and maximizing reliability and efficiency. The main functions of energy management are to provide power and voltage set points for each DG controller, to meet the balance power supply and loads, to satisfy the operational contracts with the main system, to minimize emissions, and to provide an optimal location for maximum usage of renewable sources.

In this study, optimal summation of natural power resources refers to the proper allocation and size of wind and solar power units in a grid-connected existing small grid for improved microgrid performance. The first section of this chapter introduces basic concepts of microgrid, challenges that occur in microgrid, the economic and technical model of microgrid, and the theory of distributed energy sources. The following section investigates forward-backward load flow to determine the best location of Hybrid DG in a radially modeled microgrid. The third section of the chapter discusses the formulation of an objective function while taking technical constraints into account. The theoretical underpinnings of the particle swarm optimization theorem have been discussed. The PSO was used to solve the proposed optimization function.

4.2 Microgrid Technology

The microgrid is a low-medium voltage distribution grid equipped with sensing, controlling, and communicating technology that is specifically located at consumer premises or near the load center. The advanced distribution system known as a microgrid is comprised

of a small number of distributed energy resources (DERs), both natural and/or conventional sources such as photovoltaic, wind power, hydro, internal combustion engine, micro-turbine, and gas turbine, as well as a cluster of loads [92]. Rapid advancements in power electronics and communication technology are helping to shape the microgrid. Other key features that contribute to the efficiency and dependability of microgrids are generation technologies and storage devices. The microgrid structure is depicted in Fig:4.1. This section contains a brief discussion of these technologies. [87].

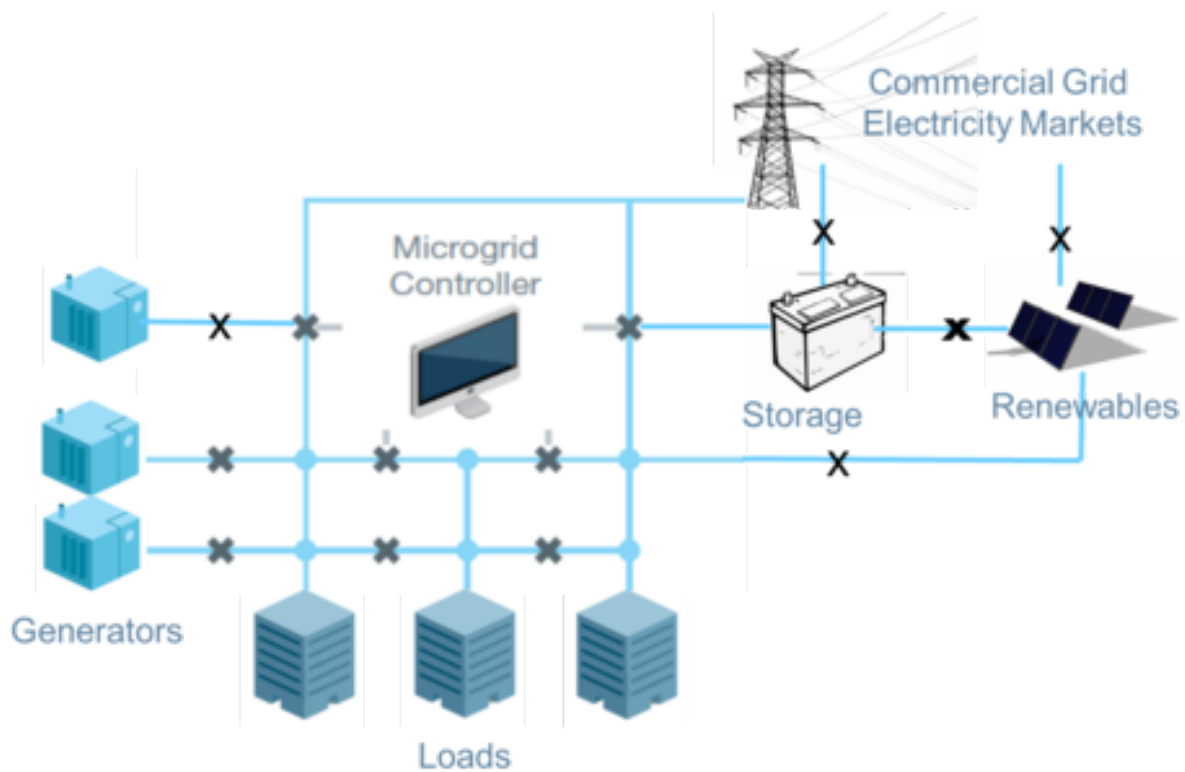


Figure 4.1: Microgrid Structure

4.2.1 Microturbines

Microturbines were previously available in a standard range of 25-100 kW. It is now possible to provide output power ranging from 25 to 250 kW, 250 to 500 kW, and up to 1000 kW at a low cost. These are single-shaft devices with airfoil bearings that operate at high speeds of 50,000-100,000 rpm. It has a simple mechanical design and relies on power electronics equipment to interface with loads. It should be suitable for clean running in Microturbines applications. The microturbines use a variety of fuels, including natural

gas, associated gas, LPG/propane, biogas, and liquid fuels (diesel, kerosene, and aviation fuel).

4.2.2 Natural Power sources

Natural power sources identified as renewable generators are part of the generating technology of Microgrids, particularly in the era of fossil fuel scarcity and global warming, and those integrated through convertors, such as 5W-5MW PV systems or wind turbines 30W-10MW. Biofueled microturbines are also classified as renewable generators. Environmentally, all natural sources are vastly superior to non-renewable combustion engines.

4.2.3 Fuel cells

Fuel cells, also known as electrochemical cells, convert the chemical energy of fuels such as hydrogen and natural gas into electrical energy. A wide range of fuel cells is available for power generation. They are very expensive, but they have low emissions and are very efficient. Transportation, special verticals, back power, portable power, electrical utility-distributed generation, space, and other applications are possible with fuel cells. Fuel cells can provide clean energy for applications ranging from one watt to several megawatts. Fuel cells of the phosphoric acid, molten carbonate, and solid oxide types are best suited for distributed generation applications. Phosphoric acid Fuel cells (PAFC) are commercially available in the 5-400-kW range, with operating temperatures ranging from 150 to 200 degrees Celsius. The main challenges of this system are expensive catalysts, a long start-up time, and sulphur sensitivity (PAFC). Major development is still going on for an alternative to these challenges.

4.2.4 Storage Devices

Renewable energy sources integrated into the grid pose a challenge in microgrid operation due to their unpredictability. The use of energy storage technology on the microgrid will ensure the supply of electric power at the specified time, provide effective generation and load balance, and ensure a better power generation plan. Flywheels, capacitor banks, supercapacitors, and batteries are the primary storage components connected to microgrid.

4.2.5 Microgrid Benefits and Challenges

The main objective of a microgrid is to provide reliable, cost-effective, and high-quality power to critical loads. It is possible to achieve this by integrating and optimizing the various energy sources. Distributed generators, which also include controlling loads, are also started referring to as DER. The emergence of DERs in microgrids provides numerous benefits to the power utility. The advantages are listed below.

- Environmental: Reduced emissions of greenhouse gases and pollution.
- Technical: Electric T&D losses reduced, Deferred electric T&D capacity investments and support for deployment of renewable generation, Enhanced power quality, reliability
- Economical: Energy cost reductions facility, provide Ancillary service in the electric market, Supply, and sell excess electricity to the main grid and other microgrids. facilitate demand response program, optimize the size of power grid assets on pricing base and real-time market base.

All of the benefits listed above are only possible if the microgrid architecture is supposed to be efficient. The technical challenges in microgrid functionality are fast controller response, a unique protection scheme required for the protection of power electronics interfaced sources and devices, energy management with power dispatch set points, and voltage control. The microgrid system should be able to operate smoothly and automatically in autonomous and grid-connected modes, as well as rapidly detect load changes and regulate the voltage at each microsource. Bi-directional current flow is a critical function for achieving microgrid benefits.

In the case of real-time energy costs, the configuration and operation of a microgrid affect the economics of energy markets. In the case of microgrid configuration and operation, the economics of optimal investment and available operation technology arrive first. This issue motivates intense academic scrutiny at the distribution system scale. Microgrid development must be such that it behaves like a legitimate customer or generator in relation to the bulk power system while also boosting traditional economic roles. However, due to its low voltage, the microgrid's ability to deliver energy beyond the substation and provide ancillary services is limited.

In this study, an algorithm has been proposed to embed natural power resources combined with microturbines in distribution systems to minimize grid losses, and the microgrid's reliance on the main grid has been examined in view of the uncertain nature of renewable resources.

4.3 Microgrid Model

The goal of incorporating natural power sources into microgrids is to upgrade existing distribution systems with optimal DER allocation. Here The radial distribution system has been modeled for microgrid deployment. The single line diagram is depicted in Fig:4.2. As shown in Fig.4.3, the distribution system is considered a microgrid, with Natural Power



Figure 4.2: Single line diagram of radial distribution system.

Distributed Generators (NPDG) such as wind and solar units installed at the bus, say i . The system has n buses indexed by $i = 1, 2, 3, \dots, n$. The main grid feeds the system through a transformer at bus 1, considered a slack bus. The distribution power flow equation is expressed before installing the NPDG is given by equation: (4.1) [93] [94]; The 'n' is a far end node.

$$P_{n-1} = P_n + r_{(n,n-1)} \left(\frac{P_n^2 + Q_n^2}{V_n^2} \right) \quad (4.1)$$

$$Q_{n-1} = Q_n + x_{(n,n-1)} \left(\frac{P_n^2 + Q_n^2}{V_n^2} \right) \quad (4.2)$$

$$V_{n-1} = (V_n) + \left(\frac{r_{(n,n-1)}P_n + x_{(n,n-1)}Q_n}{V_n^2} \right) \quad (4.3)$$

$$I_{b(n-1,n)} = \frac{S_n^*}{V_n} \quad \text{where,} \quad S_n = P_n + jQ_n \quad (4.4)$$

The voltage at any other bus i becomes;

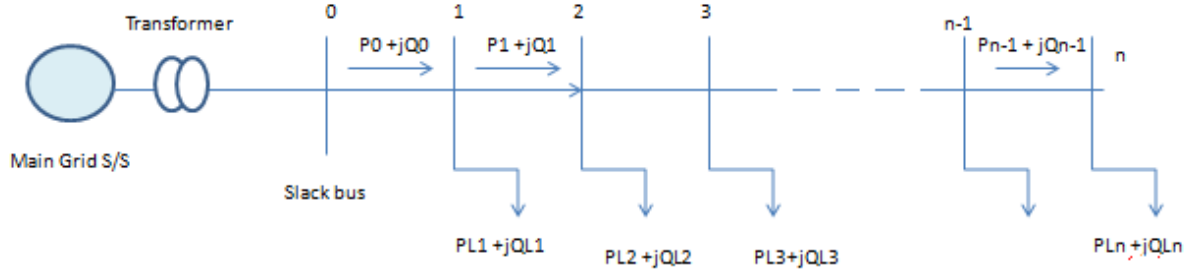


Figure 4.3: Power flow in radial distribution system.

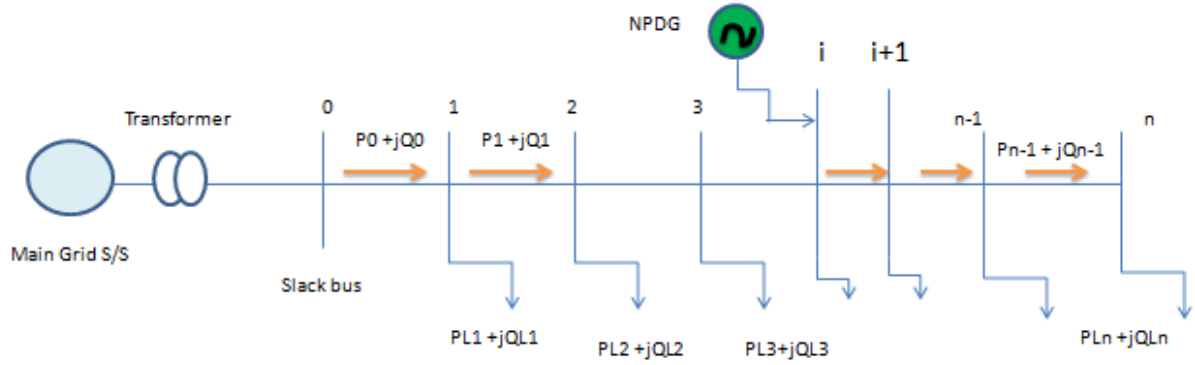


Figure 4.4: DG placement at bus i.

$$V_{(i+1)} = V_i - \left(\frac{r_{(i,i+1)}P_i + x_{(i,i+1)}Q_i}{V_i^2} \right) \quad (4.5)$$

The branch current will be;

$$I_b(i+1, i) = \frac{V_i - V_{(i+1)}}{Z_{(i,i+1)}} \quad (4.6)$$

. To find the voltage at bus 1, in backward sweep, follow these steps from the far end node to the slack bus. As shown in Fig: 4.4, the power flow expression after placement of DG at the bus k has been taken into account as per equation: (4.7). The reactive power at bus i is assumed to be balanced by reactive power sources at that bus.

$$P_{k+1} = P'_k - r_{k,k+1} \left(\frac{(P'_k)^2 + (Q'_k)^2}{V_k^2} \right) \quad \text{where} \quad P'_k = P_k + P_{DGk} - P_{Lk} \quad (4.7)$$

$$Q_{k+1} = Q'_k - x_{k,k+1} \left(\frac{(P'_k)^2 + (Q'_k)^2}{V_k^2} \right) \quad \text{where} \quad Q'_k = Q_k + Q_{DGk} - Q_{Lk} \quad (4.8)$$

$$V_{k+1} = V_k - \left(\frac{r_{(k,k+1)}P'_k + x_{(k,k+1)}Q'_k}{V_k^2} \right) \quad (4.9)$$

$$I_{b(k+1,k)} = \frac{V_k - V_{(k+1)}}{Z'_{(k,k+1)}} \quad (4.10)$$

4.4 Backward Forward Sweep Power Flow

The power flow of a radial distributed system can be solved by the backward-forward sweep method, which is based on KCL and KVL for finding branch current and node voltage. Because of radial structure and high R/X ratio, the conventional power flow methods failed to provide good results for distribution network analysis. The backward/forward sweep processes which make use of the well-known bi-quadratic equation have gained popularity for distribution systems load flow analysis due to their computational efficiency, robust convergence characteristics, and low memory requirements [95]. The power flow is executed in three steps in Bw/Fw sweep algorithm.

- Backward sweep
- Forward sweep
- Nodal analysis using Convergence criteria.

4.4.1 Backward Sweep Process

In the initial stage of power flow, assume flat voltage, i.e., set each node voltage to 1.0 pu. The effective power flow begins at the last node-n and proceeds backwards to the root node -0. The effective real power flow from node no: 1 to n can be calculated using the equation:(4.1). The reactive power can be calculated by equation:(4.2). The nodal voltage values are kept unchanged during the backward sweep. The branch power flow is updated in each iteration of a backward sweep.

4.4.2 Forward Sweep Process

The outcome of the forward propagation is to compute the voltages at each node starting from the central grid substation outgoing feeder node. The source feeder voltage is set at its actual value. During the forward sweep procedure, the effective power in each branch

is kept unchanged to the value gained in backward run. The node voltage magnitudes are computed using equation:(4.3). The branch current is also calculated in this forward walk using the equation: (4.6). The voltage angle is calculated using the equation: (4.5).

4.4.3 Nodal Analysis using Convergence Criteria

The comparison between nodal voltages calculated in the previous and present iterations is carried out to reach towards analysis. If the maximum mismatch between voltages in the successive iterations is less than the specified tolerance, the conversion has been obtained. Otherwise, new effective power flows in each branch are calculated through backward run with the present computed voltages, and then the backward-forward sweep process is repeated until the solution is converged. After the convergence, network parameters like active power and reactive power losses can be computed. This algorithm for power flow has been applied for upgradations of radial distribution system using modified power flow equation: (4.7,4.8,4.9,4.10). The objectives of upgradation are to locate NPDG, accounting for its uncertain nature, and minimize the grid's real power losses. .

4.5 Application of Backward Forward Load Flow to Radial Distribution System

For determining the grid losses, the above discussed modified distribution load flow algorithm has been applied to the radial node radial distribution system without placement of NPDG and with the placement of Solar-wind and MT as a single unit and as a hybrid unit placed at a single bus or various combination of buses. The grid real power losses are the sum of all branch losses which are given by

$$G_{loss} = \sum_{ij=1}^{n_b} I_{ij}^2 r_{ij} \quad \text{where, } I_{ij} = I_{b(k,k+1)} \quad (4.11)$$

4.5.1 NPDG data

The wind speed and solar irradiation data for the area near the seashore of Gujarat, India, has been studied to get an idea about wind speed potential and solar irradiation, as discussed in chapters 2 and chapter 3. The wind and solar models discussed in previous

chapters have been utilized as power generation limits of NPDG to place in the Distribution network. The land and geographical limitations of any area may force to decide limits of no of NPDGs. Here maximum no of NPDGs are taken three. One micro turbine of 500 KW has been considered for reliable operation of a microgrid and minimum dependency on the main substation and to avoid immediate 100% loading of a microgrid on the main grid during non-availability of natural resources. Here the discrete size of wind generation unit and solar power generation unit with the technical specification is shown in Table:4.1. The probable power generation of these NPDGs has been modeled as given in previous chapters 2 and 3.

Table 4.1: Selected size of NPDG

wind based NPDG	solar based NPDG	micro turbine
Rated power :2.1 MW Rated speed :11 m/s Cut-in speed:3.5 m/s Cut-out speed: 25m/s hub height :79 m	rated Power: 100MW No of module: 250wp module capacity: 400 nos system losses : 28%	rated Power: 500MW rated voltage :4.15KV

4.5.2 Network and Load Data

The IEEE -13 node radial distribution system has been used as a microgrid for the implementation of the proposed method. The Fig.4.5 shows 13 node radial distribution system [96]. The bus data and line data with renumbering of the node is mentioned in Appendix A. This system is supplied by 115/4.16 KV, 5000 KVA substation. System is small but highly loaded with an unbalanced spot and distributed load. Here system per phase spot load at the end of feeder line is modeled as constant PQ load, Z load and I load as given in [96]. The distributed load at node 632 is also considered a spot load. The unbalanced 3-phase distributed load and spot load is converted into 3-phase balanced load. Here, Load per phase has been considered for analysis purpose. The transformer between node 633 and node 634 is considered as a unity gain isolated transformer. The total connected load of the system is 1760.7 KW. The maximum feeder current limit is 1KA. Total network losses computed after forward backward load flow are: 19.63 KW without DG Placement.

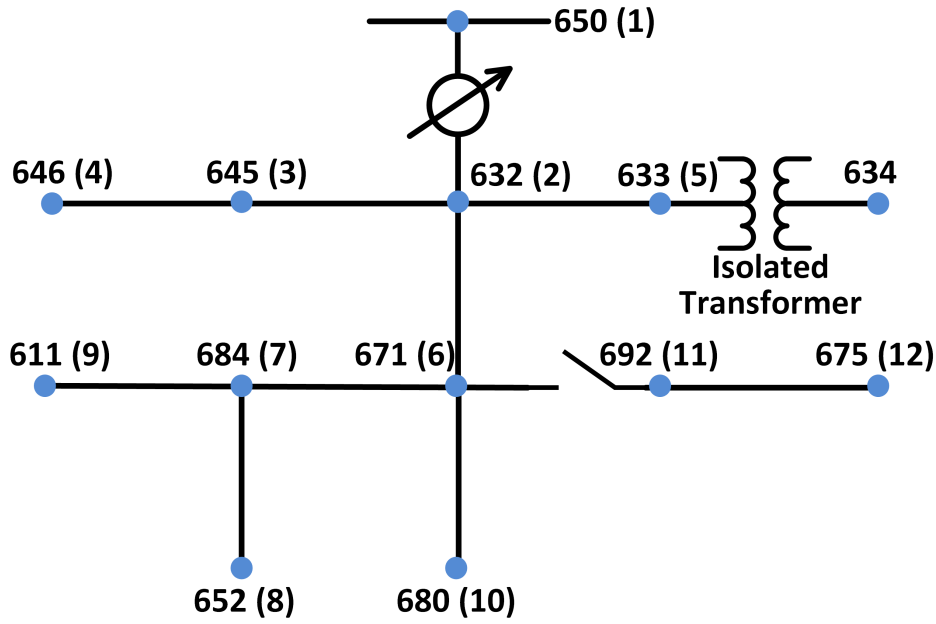


Figure 4.5: Single line diagram of IEEE-13 node system with renumbering

Here for study purpose, one year has been divided into four seasonal time laps; winter, summer, spring, and fall. The 24-hours seasonal system active power load and reactive power load profile are assumed to IEEE RTS model. This system provides weekly peak load as a percentage of the annual peak load, daily peak load cycle as a percentage of the weekly peak, and hourly peak load as a percentage of the daily peak load. A typical daily load profile for each period has been generated as a percentage of the annual load as given in [60],[97]. The hourly average load over one day has been generated as a percentage of peak load by computing the average of daily load profile over 24 hours.

4.6 Application of Backward Forward Load Flow on IEEE 13 node Distribution System for placement of NPDG

. The BF load flow has been primarily run in the Matlab platform to obtain node voltage, branch current, and active power losses in the IEEE 13 node distribution system. The hourly average load over the day as a percentage of peak load for each time-lapse has

been taken for load flow consideration. The seasonal, hourly average load of the system has been given in Table: 4.2. The following steps have been incorporated in power flow

Table 4.2: Seasonal hourly average load

season	system load in kw
winter	1037
summer	1459
spring	920
fall	865

algorithm for NPDG placement.

- Read bus data and line data of the radial distribution system
- Run BF load flow considering hourly average load over the day for each season and noted node voltages, branch current and total branch current losses using Eq.4.11 for the system without placement of DG
- Run load flow for all placement combinations say; $\binom{n}{r}$. where, n= number of buses and r= The discrete number of NPDG units and one microturbine, and obtain load flow result for node voltages, branch current and total branch current losses. The chosen number of NPDG units has been mentioned in Table: 4.3
- Buses at which minimum branch current losses occur are considered as best placement for NPDG combination

The result of load flow for each combination of NPDG best placement is shown in Table: 4.4

4.6.1 Load Flow Result and Discussion

The analysis was carried out based on the results. Table:4.4 shows that when only two NPDGs are chosen for placement, Bus nos. 4 and 7 are the best locations for NPDG placement. Using NPDG combination as per case 1, losses were reduced up to 35 percent to 50 percent in each season and 25 percent in case 2. If three NPDGs are chosen, and the combination shown in Case 3 is used, the third-best placement is bus number 12, and

Table 4.3: Combination of NPDG

Combination set cases	solar based NPDG	wind based NPDG	micro turbine
Case 1	1	0	1
case 2	0	1	1
case 3	0	2	1
case 4	1	1	1
case 5	1	2	1
case 6	0	3	1
case 7	3	0	1

losses are reduced up to 20% to 25% in each season. Bus numbers 4,3/10,12,6 are the best locations for the placement of four NPDG scheduled, with a reduction in losses up to 10% to 20% in each season.

It is concluded that the best location of the NPDG set for total branch losses reduction can be determined based on NPDG's hourly average power generation and the grid's hourly average seasonal load. Aside from that, the most heavily loaded node should be secured in order to ensure reliable power generation via microturbines. Nodal voltage and branch current are within limits in each case. In this analysis, excess power is delivered by the substation in the event of low NPDG power generation. In some cases, when NPDG's power generation exceeds load, the excess power is not examined in this section. The flow of current has only been considered in one direction. The probable power generation of natural power sources and the maximum power generation limit of MT has been considered as negative loads in a microgrid for optimal placement of DG to fulfill objectives such as minimizing losses and node voltage constraints. This method is pessimistic and time-consuming for NPDG integration in the microgrid. To overcome the limitations of this conventional method, a new problem strategy for the optimal summation of natural power distributed generators has been developed.

4.7 Problem Formation Strategy and Solution

The main aim behind the summation of natural distributed power resources is to determine the location and sizing of solar power panels and wind generators in small distribution systems as a microgrid in order to minimize real power losses. Another goal, in addition to minimizing losses, is to run the microgrid autonomously for an extended period. In this case, autonomous mode means that the incoming current flow from the main substation is zero. To enable autonomous mode, conventional MicroTurbines (MT) must be integrated with natural power resources. Relying solely on natural sources creates reliability and stability issues with voltage and frequency. [98]. In summary, technical and environmental benefits in any robust planning imply a reduction in technical losses with maximum utilization of natural power. Fig:4.6 shows block representation for the steps for the strategy of optimal summation of Natural Distributed power sources (NDPS). The total network power losses, which are dependent on system parameters, can be calculated using one of three methods described in [47]. For problem formation, the branch current loss approach has been used. Total network losses per given time laps have been reduced by optimising the placement of natural power distributed generation.

4.7.1 Objective Function

Network total real power losses have been computed as per this formula 4.11 introduced as objective function I.

$$OF_1 = \sum_{ij=1}^{n_t} N_{loss}^t \quad (4.12)$$

The main substation dependency factor (DF) has introduced for the analysis of power feed from the grid during periods of non-availability or low power availability of wind and solar, as well as power injected into the grid during excess generation of NPDG . It is defined as a percentage of power supply from the main substation (s_p) when compared to supply from NPDG units and microturbines. Another consideration for natural power unit allocation is to maximise the participation of available wind and solar units for given time interval. The formula for main substation dependency factor has been expressed as; (4.13) and is introduced as objective function II.

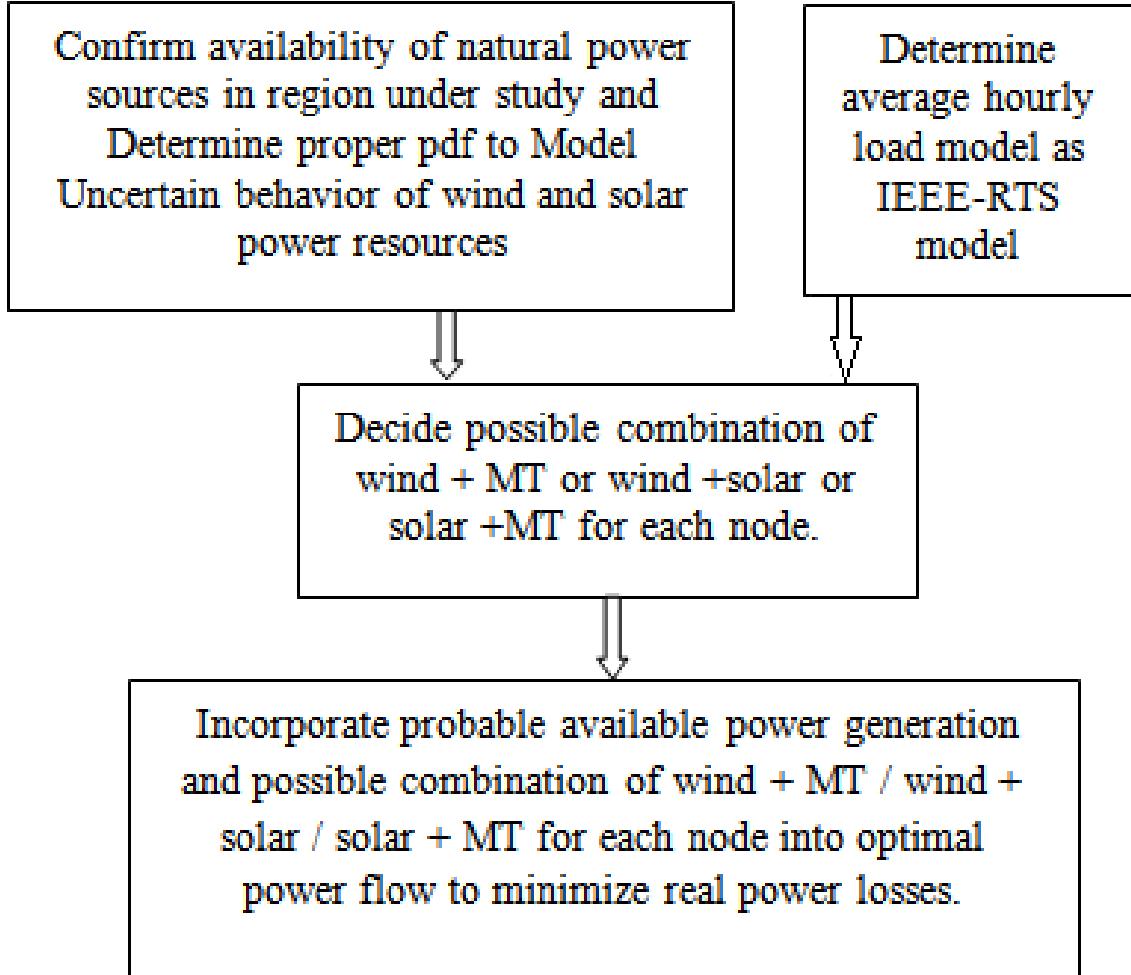


Figure 4.6: Block representation of problem formation strategy for optimal summation of Natural Power Distributed Generators

$$OF_2 = DF^t = \frac{\frac{s_p}{P_D}(t)}{-\sum_{ij=1}^{n_d} \frac{P_{npdg_i} + P_{mt_i}}{P_D}} * 100 \quad (4.13)$$

Here, " P_{npdg_i} " is power generation of NPDG and " P_{mt_i} " power generation of microturbine for given time lapse. " P_D " is microgrid power demand for given time lapse, " N_d "- no of nodes. The constraints which have been included in objective function as follows:

- 1) Nodal voltage constraints

$$V^{min} \leq V_i \leq V^{max} \quad (4.14)$$

2) Feeder current flow constraints: Feeder current passing through each branch is not permissible to violate from the allowable limit. During low load period, there may be possibility of reverse power flow due to downstream higher DG power generation

$$-I^{max}(I^{max}) \leq I_{ij} \leq I^{max} \quad (4.15)$$

3) Power generation limits of NPDG

$$P_{WG} = \sum_{i=1}^{N_d} n_{wgi} * P_{wratedi};$$

where,

n_{wgi} = no of possible wind unit; $P_{wratedi}$ = wind unit rated capacity;

$$P_{SG} = \sum_{i=1}^{N_d} n_{sgi} * P_{sratedi};$$

n_{sgi} = no of possible solar unit; $P_{sratedi}$ = solar unit rated capacity;

$$P_{MTG} = \sum_{i=1}^{N_d} n_{mtgi} * P_{mtratedi}$$

where,

n_{mtgi} = no of possible microturbine unit; $P_{mtratedi}$ = microturbine unit rated capacity;

The multi-objective function which is formulated by summation of OF_1 , OF_2 and constraints. It has been transformed into the single objective function. The single objective function has been obtained using equal weighted least square conversion. It is shown in Eq:4.16.

$$F = OF_1^t + OF_2^t + ((V_i)^{max} - (V_i))^2 + ((V_i) - (V_i)^{min})^2 + ((I_{ij})^{max} - (I_{ij}))^2 + ((I_{ij}) - (I_{ij})^{min})^2 \quad (4.16)$$

4.7.2 Optimisation Problem Solution and Discussion

Many methodologies are available for solving optimization problems, as discussed in chapter 1. Here Particle swarm optimization (PSO) technique is used to solve the proposed optimal problem. For one decade, PSO has been the most popular method with high-speed

convergence and fewer computation advantages. It solves optimization problems by iteratively and having ‘n’ no of particles that present candidate solutions. For multi-objective problems, the ‘m’ is no of optimized variables. These optimized variables indicate the dimension of the problem. Description of PSO algorithm with its merits has been presented in [50],[51][99].

The wind unit and solar unit models discussed in Chapters 2 and 3 were used to calculate the probable hourly average generating power. The maximum generating limit of the natural power resource unit has been set at the probable hourly average generating power value. The Matlab coding has been finished in such a way that PSO can be applied to each of the cases listed in Table: 4.4, and a final result, as well as intermediate results for cases 5,6 and 7, have been obtained.

It is discovered that optimization has been achieved for the set of four NPDG when placed at nodes 4, 7, 10, and 13. This is the best and most effective combination. It has been proven that when placement of any combination of four DGs on these buses has given minimal losses. Instead of executing the program one by one for each combination, this best optimal combination has been directly achieved using PSO. For minimal losses and minimal reliance on the main grid, a larger DG is required to be placed at the heavily loaded node.

The optimum combination for all season is shown in Table:4.5 through 4.7. When wind power potential is good and geographical conditions permit its use, case:6 appears to be the best optimal combination. The Epoch versus g_{best} graph for the spring season is shown in Fig:4.7. This combination provides the best value for each season.

When both wind and solar units are available, case no:5 is used, and Table: 4.6 shows the microturbine placement and optimal unit generation needed to reduce losses and DF. Solar power is available for daytime only, so power generation is insufficient for a 24-hours-based hourly average load. Because a large solar power unit necessitates a large land area, Case 7 is rarely encountered. In this case, it became attempted to achieve optimization with a 100 KW power 3nos solar panel. When only solar generation is possible due to geographic conditions, the placement nodes and optimum generation units are identified and listed in Table:4.7.

Fig:4.8 and Fig:4.9 show Epoch versus g_{best} graph for the spring season with case 5 and case 7 placement, respectively. For all three cases, the results of optimization methods such as Gbest, the optimum value of system losses, and s/s dependency factor have been

shown in Table:4.8. Network seasonal losses have been significantly reduced with the placement of natural power resources. The substation dependency factor is higher in the winter due to low wind power generation. In contrast, in the spring and fall seasons, when an hourly average load is less than the hourly average generation, the microgrid feeds power to the main grid, resulting in a negative s/s dependency factor. In cases 6 and 7, the branch power flow after placement of NPDG is within limits, as shown in Fig: 4.10. The hourly average generation of the sum of wind and MT is higher than the hourly average load during the spring and fall seasons, indicating reverse current flows in branch one and a negative substation dependency factor, indicating power injection in the substation.

4.8 Conclusion

This chapter is presented a microgrid power flow analysis with backward-forward distribution load flow. It also presented the development of an optimal problem strategy for determining the placement and size of NPDG and microturbines in the grid-connected microgrid. The hourly average probable power generation of wind and solar units has been taken into account as the maximum power generation limit of that unit for the reliable operation of a distributed power system. The optimal summation has been determined based on the hourly average load and hourly average probable generation. In order to minimize losses and reliance on the main grid, the highest loaded node is the best optimum location for any DG having a maximum power generation limit. This problem strategy can also be applied on a 24-hours basis and real-time basis by considering hourly probable power generation and load. The optimal scheduling can also be planned on the basis of this strategy and the probable power calculation of NPDG. A better and more speedy result has been obtained using the Particle Swarm Optimisation technique. The proposed method has been verified on IEEE-13 bus distribution system.

Table 4.4: Optimal placement of DG for Each Combination of NPDG.

season	NPDG set cases	best place- ment	G_{losses} without NPDG place- ment	G_{losses} after NPDG place- ment
winter	case 1	4,6	5.37	2.09
	case 2	4,6		1.71
	case 3	12,4,6		1.245
	case 4	12,4,6		1.55
	case 5	12,3,4,6		1.21
	case 6	12,9,4,6		0.535
	case 7	12,9,4,6		0.936
summer	case 1	4,6	10.92	5.34
	case 2	4,6		3.27
	case 3	12,4,6		2.04
	case 4	12,4,6		4.19
	case 5	4,3,7,12		1.19
	case 6	12,3/9,4,6		0.65
	case 7	12,3,4,6		3.436
spring	case 1	4,6	4.23	1.42
	case 2	4,6		1.03
	case 3	12,4,6		0.87
	case 4	12,4,6		1.69
	case 5	4,3/9,6,12		0.79
	case 6	12,3,4,6		0.345
	case 7	12,3,4,6		0.986
fall	case 1	4,6	3.74	1.33
	case 2	4,6		0.94
	case 3	12,4,6		0.86
	case 4	12,4,6		1.01
	case 5	4,3,12,6		0.97
	case 6	12,3/9,4,6		0.325
	case 7	12,3/9,4,6		1.0593

Table 4.5: Optimal Placement of DG for Case 6 using PSO.

season	best placement node no with hourly average power generation re- quired in kW				Details DG placement
	4	6	3/9	12	
Winter	180	319	180	180	wind unit at node 4,9,12
Summer	327	500	211	277	MT unit at node 6
Spring	217	343	133	226	wind unit at node 4,3,12
Fall	211	290	143	251	MT unit at node 6

Table 4.6: Optimal placement of DG for Case 5 of NPDG using PSO

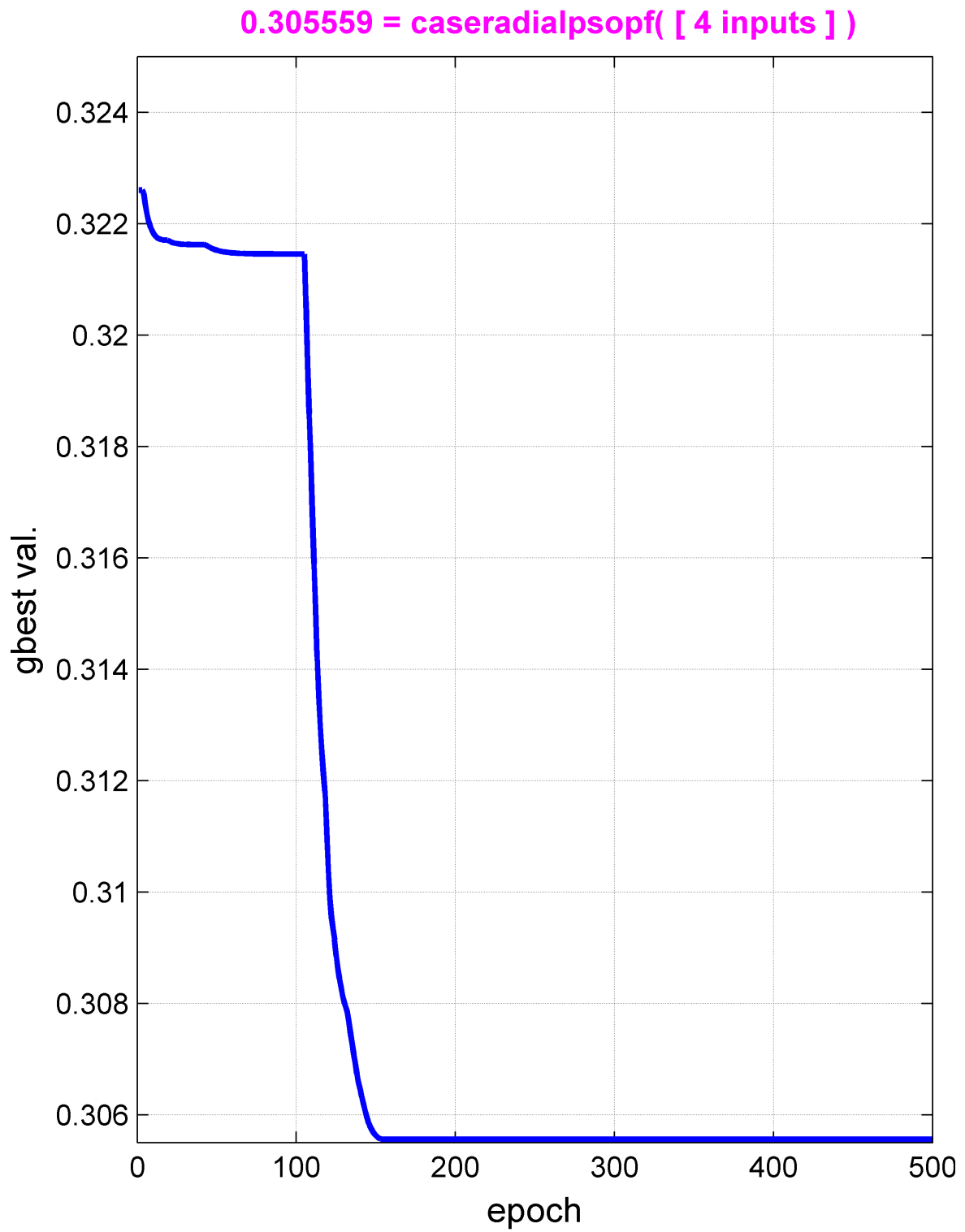
season	Best placement node NO with hourly aver- age power generation required in kW				Details DG placement
	4	6	3/9	12	
Winter	180	500	180	45.63	wind unit at node 4,12 Solar at
Summer	417.9	500	288.5	44.7	node 3, MT unit at node 6
Spring	202.9	470.4	133.2	42.3	wind unit at node 4,12 Solar at
Fall	253	432	125	19.8	node 9, MT unit at node 6

Table 4.7: Optimal placement of DG for case 7 of NPDG using PSO.

season	Best placement node NO with hourly aver- age power generation required in kW				Details DG placement
	4	6	9	12	
Winter	45	500	45	45	solar unit at node 4,9,12 MT unit at node 6
Summer	60	500	60	60	
Spring	40	500	40	40	solar unit at node 3,4,12 MT unit at node 6
Fall	15	500	15	15	

Table 4.8: Value of Optimised Function.

seasonal Time Lapse	g_{best}			S/S dependency factor			G_{losses} in KW		
	solar MT	wind MT	wind solar MT	solar MT	wind MT	Wind solar MT	solar MT	wind MT	Wind solar MT
winter	1.8849	0.7769	1.166	0.6335	0.1719	0.2275	0.773	0.45	0.5356
summer	4.5650	0.6638	1.4965	1.1469	0.0292	0.1430	3.4182	0.6346	1.93
spring	1.427	0.3056	0.6183	0.4849	-0.032	0.078	0.9421	0.3374	0.69
fall	6.334	0.2912	0.6277	0.5876	-0.034	0.409	1.0493	0.3256	0.6389

Figure 4.7: G_{best} with wind unit placement in Spring season

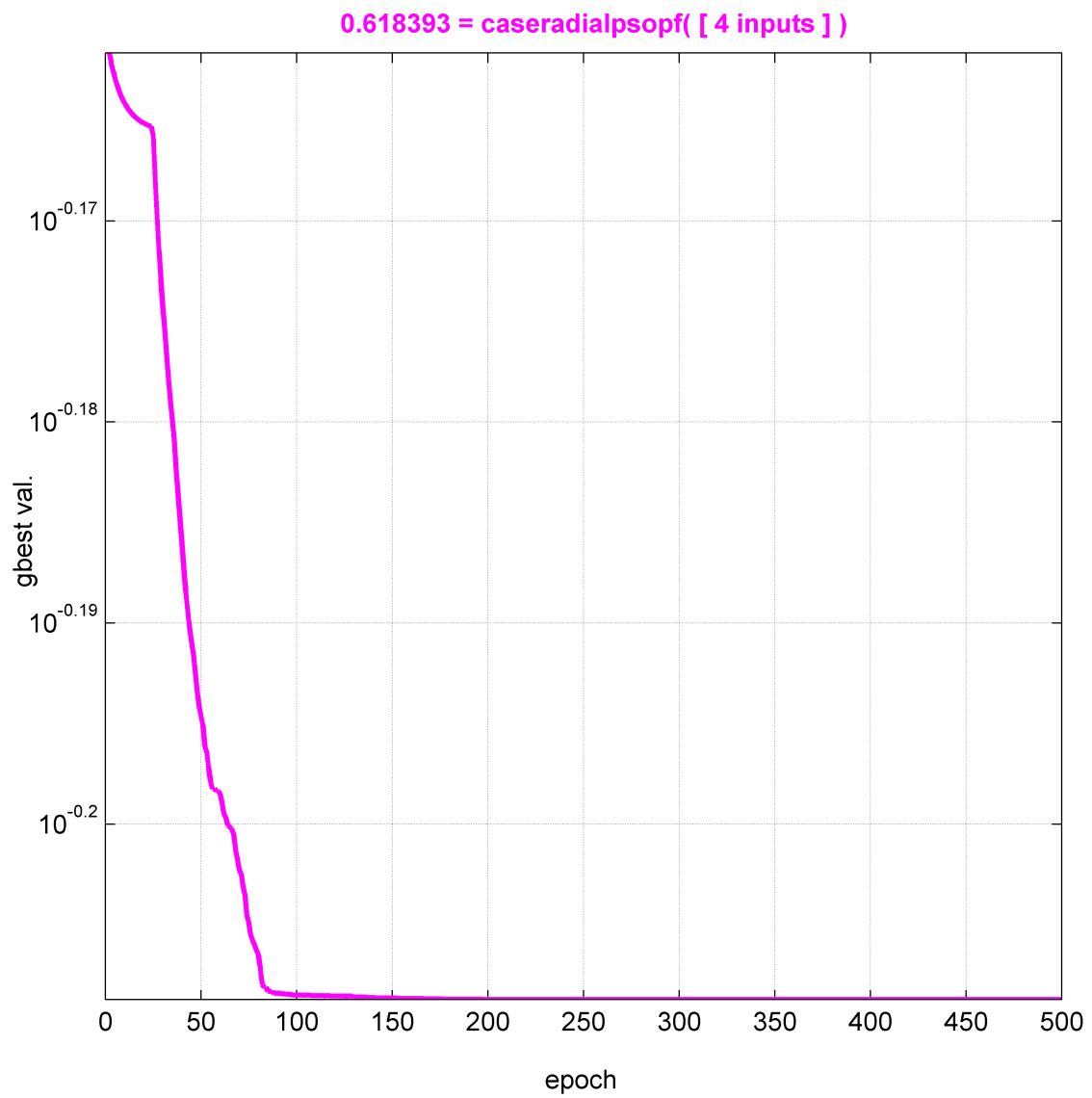
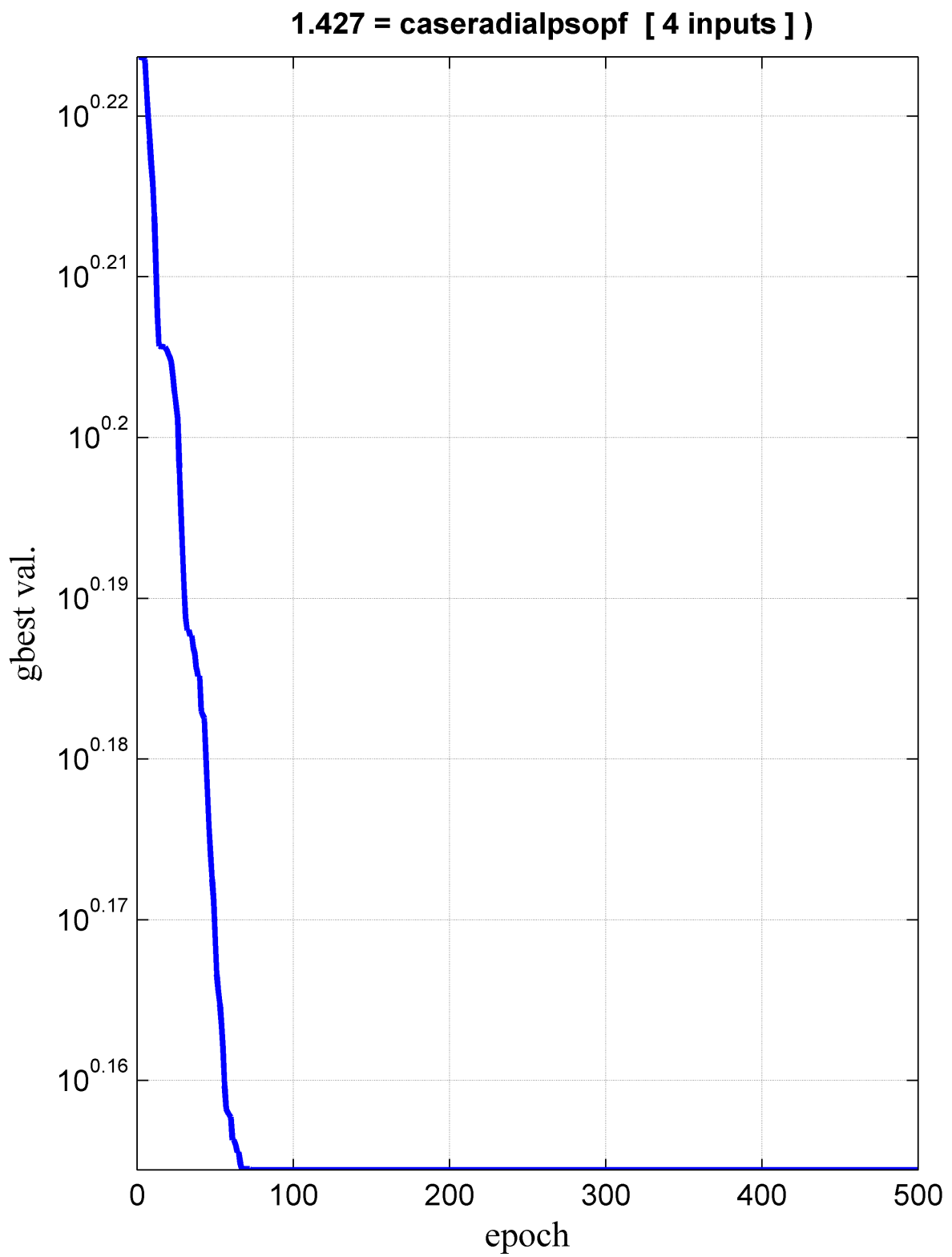


Figure 4.8: G_{best} with wind and solar unit placement in Spring season

Figure 4.9: G_{best} with solar unit placement in Spring season

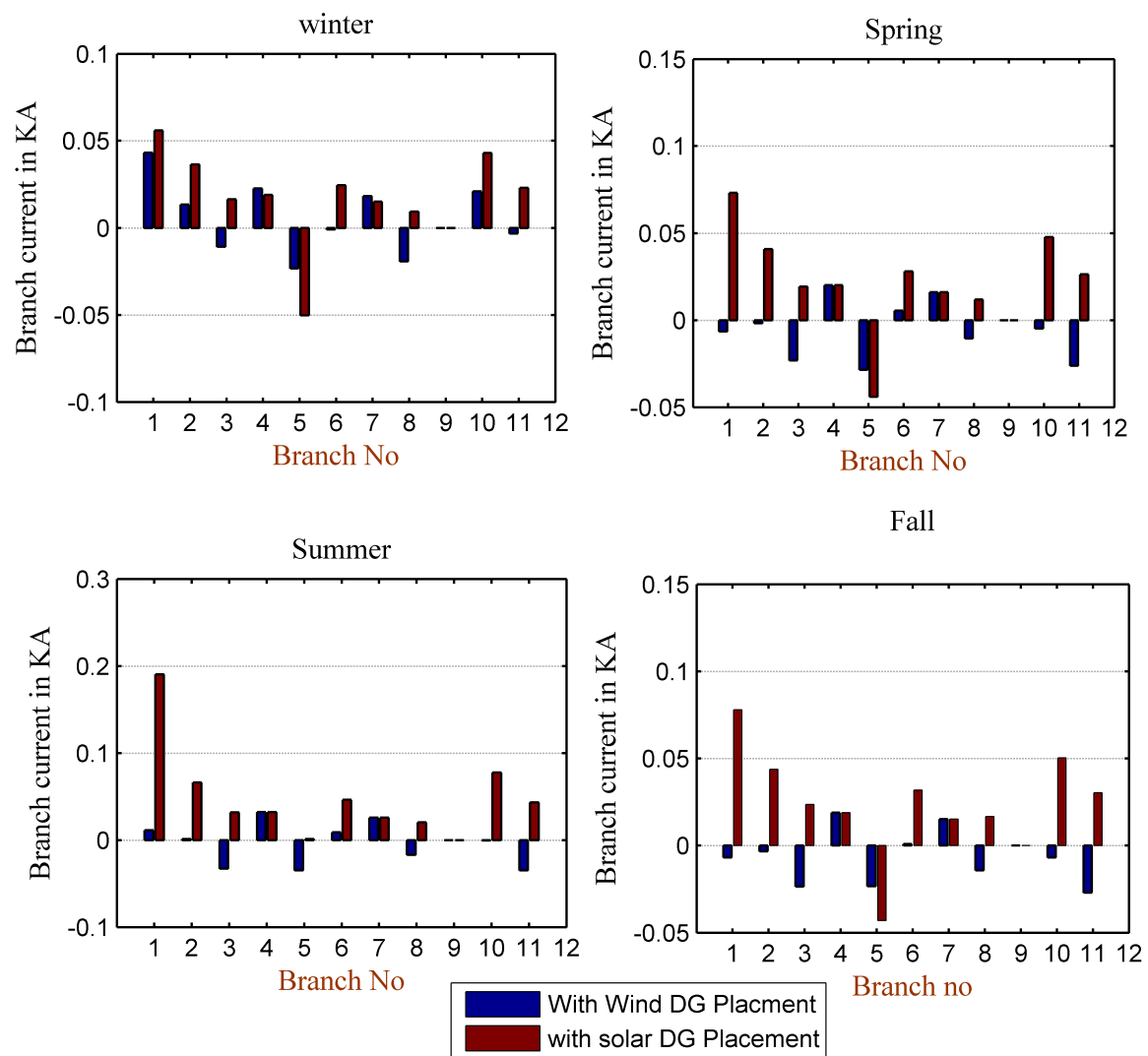


Figure 4.10: Reverse current flow in case 6